

# UC Berkeley

## UC Berkeley Previously Published Works

### Title

The Spatial Frequency Content of Urban and Indoor Environments as a Potential Risk Factor for Myopia Development

### Permalink

<https://escholarship.org/uc/item/317418ht>

### Journal

Investigative Ophthalmology & Visual Science, 61(11)

### ISSN

0146-0404

### Authors

Flitcroft, Daniel Ian

Harb, Elise N

Wildsoet, Christine Frances

### Publication Date

2020-09-28

### DOI

10.1167/iovs.61.11.42

Peer reviewed

# The Spatial Frequency Content of Urban and Indoor Environments as a Potential Risk Factor for Myopia Development

Daniel Ian Flitcroft,<sup>1,2</sup> Elise N. Harb,<sup>3</sup> and Christine Frances Wildsoet<sup>3</sup>

<sup>1</sup>Ophthalmology, Children's University Hospital, Dublin, Ireland

<sup>2</sup>Technological University of Dublin, Dublin, Ireland

<sup>3</sup>School of Optometry, University of California, Berkeley, California, United States

Correspondence: Daniel Ian Flitcroft, Children's University Hospital, University College Dublin, Temple Street, Dublin, D1, Ireland; [ian@flitcroft.com](mailto:ian@flitcroft.com).

Received: June 30, 2020

Accepted: September 7, 2020

Published: September 28, 2020

Citation: Flitcroft DI, Harb EN, Wildsoet CF. The spatial frequency content of urban and indoor environments as a potential risk factor for myopia development. *Invest Ophthalmol Vis Sci.* 2020;61(11):42. <https://doi.org/10.1167/iov.61.11.42>

**PURPOSE.** To examine the hypothesis that the spatial frequency spectra of urban and indoor environments differ from the natural environment in ways that may promote the development of myopia.

**METHODS.** A total of 814 images were analyzed from three datasets; University of California Berkeley (UCB), University of Texas (UT), and Botswana (UPenn). Images were processed in Matlab (Mathworks Inc) to map the camera color characteristics to human cone sensitivities. From the photopic luminance images generated, two-dimensional spatial frequency (SF) spectra were calculated and converted to one-dimensional spectra by rotational averaging. The spatial filtering profile of a 0.4 Bangerter foil, which has been shown to induce myopia experimentally, was also determined.

**RESULTS.** The SF slope for natural scenes followed the recognized  $1/f^x$  relationship with mean slopes of  $-1.08$ ,  $-0.90$ , and  $-1.04$  for the UCB, UT and UPenn image sets, respectively. Indoor scenes had a significantly steeper slope ( $-1.48$ , UCB;  $-1.52$ , UT;  $P < 0.0001$ ). Urban environments showed an intermediate slope ( $-1.29$ , UCB;  $-1.22$ , UT) that was significantly different from the slopes derived from the natural scenes ( $P < 0.0001$ ). The change in SF content between natural outdoor scenes and indoors was comparable to that induced by a 0.4 Bangerter foil, which reduced the SF slope of a natural scene from  $-0.88$  to  $-1.47$ .

**CONCLUSIONS.** Compared to natural outdoor images, man-made outdoor and indoor environments have spatial frequency characteristics similar to those known to induce form-deprivation myopia in animal models. The spatial properties of the man-made environment may be one of the missing drivers of the human myopia epidemic.

Keywords: myopia, form deprivation, spatial frequency, visual environment

There is ample evidence that the prevalence of myopia is increasing globally.<sup>1</sup> Although a range of risk factors, such as education and near work, and protective factors, including time outdoors, have been identified, currently available interventions do not consistently prevent the development of myopia.<sup>2-5</sup> Certain features of human myopia also remain unexplained, such as the reasons why urban living appears to be an independent risk factor for myopia development.<sup>6,7</sup> Population density and the type of housing also appear to be relevant factors.<sup>8,9</sup> Despite the common assertion that light levels explain the protective effect of time outdoors, it remains unexplained why some countries, such as Norway, with low seasonal light levels and high levels of near work have low levels of myopia.<sup>10</sup> A Taiwanese study promoting increased outdoor time during school found a difference in myopia progression, but objectively measured light exposure was not significantly different in the two groups.<sup>11</sup> Demonstrating that being outdoors has a protective effect against myopia also implies that being indoors

promotes myopia development, but what aspects of the indoor environment are responsible remains to be identified.<sup>12-14</sup>

There is general agreement that the current myopia epidemic has developed too rapidly to reflect any genetic changes within the population and therefore must be primarily environmentally driven. Compared to the high prevalence of myopia seen in most industrial and post-industrial societies, very low rates of myopia (<5%) are found in indigenous communities retaining their traditional cultures, based in the natural environment, with relatively little or no formal education.<sup>15</sup> Understanding what features of the modern indoor and urban environments promote myopia, and what features of the natural environment are protective may hold the key to new, more effective interventions.

In considering the role of visual environmental factors in the context of myopia, a logical starting point is the extensive body of animal research on myopia and eye growth

regulation.<sup>16</sup> The two principal models for inducing myopia, form deprivation myopia (FDM) that involves rearing animals with translucent diffusers, and lens-induced myopia (LIM) that involves rearing animals with negatively powered lenses, have been validated across a wide range of species,<sup>16</sup> implying conservation of these processes during evolution.

Of the above two models, the bidirectional defocus driven mechanism that underlies LIM (here driven by imposed hyperopic defocus), is generally assumed to be the same mechanism(s) by which a young eye outgrows its neonatal refractive error to achieve optimal focus in humans and other species, a process often termed *emmetropization*.<sup>17</sup> In FDM, degradation of spatial vision is the trigger for accelerated ocular elongation.<sup>18</sup> Apart from clinical pathologies, typically affecting the cornea or lens in infants, form deprivation is often regarded as not being relevant to human myopia. Indeed, one review noted that “there is no deprivation of form vision in the environment of the school-aged child as severe as that required to induce myopia in animals.”<sup>19</sup> However, this argument ignores its apparent evolutionary conservation, which indicates a useful biological role. Because most newborn animals are significantly hyperopic, and furthermore the mechanism for defocus-driven eye growth has a defined operating range,<sup>20</sup> this deprivation-driven mechanism could plausibly represent a back-up system to the former defocus-driven mechanism, to bring such neonatal refractive errors into its operating range.

In relation to the role of spatial frequency, it has been found in animal studies involving FDM that even relatively modest reductions in retinal image quality can elicit myopia growth responses in a range of species including chicks, guinea pigs, and primates.<sup>21–25</sup> This point is best demonstrated in studies using Bangerter foils, which filter out spatial frequencies at moderate to high spatial frequencies for the lighter density foils.<sup>25,26</sup> If similar, modest reductions of spatial frequency (“detail”) occur within modern urban and indoor environments, then a contribution from the retinal mechanism underlying form deprivation myopia may be one of the unrecognized drivers of the human myopia epidemic.

When considering key differences in the spatial frequency content of visual environments, the first step is to determine what represents a “normal” spatial profile. Images of the natural world have been found to display a remarkably consistent spatial frequency spectrum, such that the spectral amplitude (amount of contrast at a given spatial frequency) decreases with increasing spatial frequency ( $f$ ), following a relationship where amplitude is proportional  $1/f^\alpha$ .<sup>27</sup> When these two parameters are plotted logarithmically, the result is generally a straight line with a slope ( $\alpha$ ), close to  $-1.0$ , although it has been shown to vary between images from  $-0.8$  to  $-1.5$ .<sup>28</sup> This mathematical relationship indicates scale invariance in natural images and may reflect the fractal properties of many aspects of the natural world, including clouds, rocks and trees.<sup>29</sup> On the other hand, the man-made environment is structurally very different to natural environments. Modern architecture and design tend toward uniformity. Most notably, interior architecture is deficient in the fine detail that is so common in natural scenes and so is predicted to be lacking in higher spatial frequencies. These observations led to the study reported here, which investigated the hypothesis that urban and indoor environments show high spatial frequency deficiencies similar to

that known to induce form deprivation in animal models. To this end, we compared the spatial profiles of natural, urban, and indoor environments.

## METHODS

### Source of Images for Analysis

A total of 814 images were analyzed from three separate datasets. The first set (referred to henceforth as Berkeley,  $n = 155$ ) was collected by the authors in and around the University of California Berkeley (UCB) campus using a mobile phone camera (Apple iPhone 6). For validation and to remove any possible selection bias, two other high-resolution image sets were obtained from open access depositories of images for research purposes: the Natural Scene Statistics in Vision Science from the University of Texas (UT), captured with a Nikon D700 Digital SLR camera (Nikon, Inc., Tokyo, Japan) fitted with a Sigma 50 mm 1:2.8 DG Macro lens (Texas,  $n = 594$ ),<sup>30,31</sup> and the Botswana Natural Image Database album cd01A, from University of Pennsylvania (UPenn), captured with Nikon D70 (Nikon, Inc., Tokyo, Japan) fitted with an AF-S DX Zoom-Nikkor 18–70 mm f/3.5–4.5G IF-ED lens (Botswana,  $n = 65$ ).<sup>32</sup>

### Image Classification

Images were classified as natural if they contained no identifiable man-made elements. The Berkeley dataset was classified by one of the authors prior to image analysis into the following subsets: natural, mixed urban (buildings and vegetation), urban (with no obvious vegetation) and indoors. The Texas dataset was pre-classified as natural scenes, campus scenes and man-made scenes, the latter being further divided into outdoor and indoor man-made datasets for this analysis. The Botswana dataset represents a set of natural images thought to represent the visual environment in which humans originally evolved in Botswana, Africa.

### Spatial Frequency Analysis

Spatial frequency analysis was performed in Matlab (Mathworks, Inc., Natick, MA, USA) with custom software. Source images were either JPEG format (Berkeley dataset), or RAW camera images (Texas and UPenn datasets). Images were all converted into CIE (Commission Internationale de l'éclairage) LMS color space, corresponding to long-, medium-, and short-wave sensitive cones, from the manufacturer's defined color space of the different camera systems (iPhone, Nikon D70 digital SLR, and Nikon D700 digital SLR). This transformation allowed creation of images weighted according to the human photopic luminosity function. Gamma correction, where present, was reversed to create linear image files for analysis. After these steps, the source images were all subject to identical preprocessing. Images were first cropped to a square format and resized to  $1024 \times 1024$  pixels for computational efficiency. The field of view of each camera system/lens combination, adjusted for the square image format, was used to calculate spatial frequency in cycles/degree of visual angle. A fast Fourier transform (FFT) was applied to each plane of the LMS images to generate a spatial amplitude spectrum. The spectrum was then radially averaged to generate a single amplitude spectrum representing the average of each directional meridian

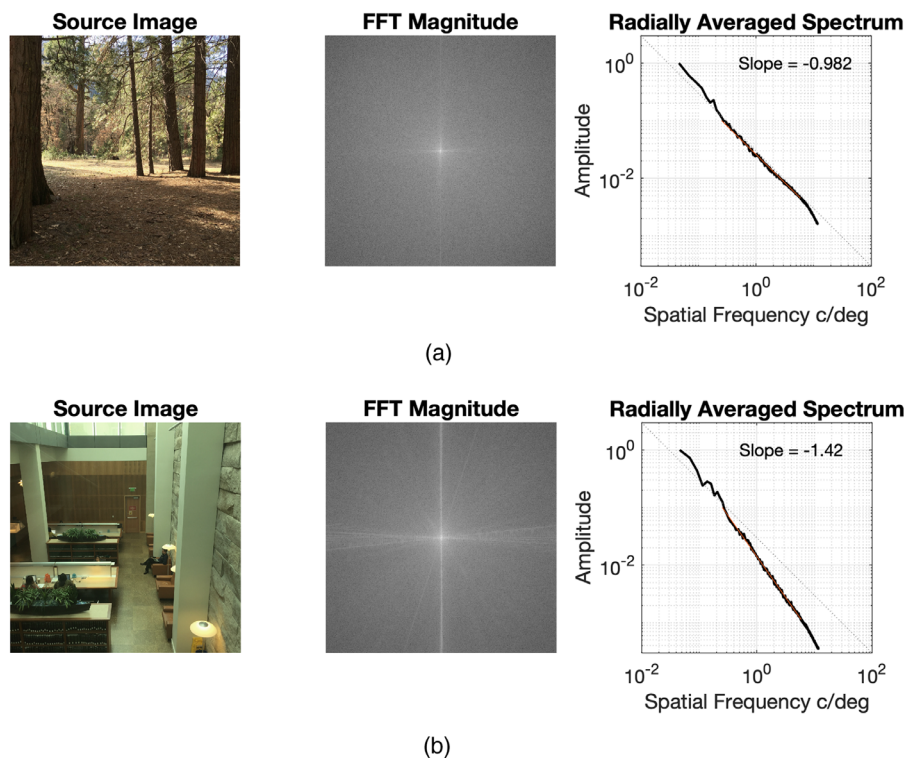


**FIGURE 1.** Spatial analysis of images showing the source image (*left*), the two-dimensional FFT (*center*), and the amplitude versus spatial frequency spectrum (*right*). For a natural scene image (**a**) the slope ( $\alpha$ ) of the log (amplitude) to log (spatial frequency) relationship is  $-0.98$ . For an indoor image (**b**) the slope of the log (amplitude) to log (spatial frequency) relationship is  $-1.42$ .

within the image. Linear regression was used to calculate the slope of the relationship between log amplitude and log spatial frequency.

### Luminance Estimation from Images

Photographic parameters, including exposure time, aperture setting and equivalent film speed (ISO) were extracted from the Exchangeable Image File (EXIF) data for each image in the datasets. Traditionally in photography, scene luminance or illuminance is used to choose appropriate aperture and exposure settings. As automatic exposure settings were involved, the reverse calculation was used to estimate scene luminance ( $\text{cd}/\text{m}^2$ ) and illuminance (lux) from the ISO, aperture, and the equivalent film ISO settings.<sup>33</sup>

### Artificial Reduction in Spatial Frequency Content of Images

In two previous studies, a 0.4 Bangerter foil proved effective in inducing myopia in guinea pigs<sup>22</sup> and also in monkeys, albeit with more variable responses.<sup>23</sup> To evaluate the impact of this Bangerter foil on the spatial frequency of a scene, images of the same scene were captured with and without a 0.4 Bangerter foil in front of the camera lens. The spatial frequency amplitude spectra of these images were calculated, as described above, and the empirical MTF calculated from the ratio of the spatial frequency amplitudes at each frequency.

## RESULTS

### Image Set Spatial Frequency Analysis

Examples of images and results of analyses are shown in [Figure 1](#) for a natural outdoor and an indoor image. Both images display the expected relationship between spatial frequency and amplitude: the spectral amplitude is proportional to  $1/f^\alpha$  in both cases, differing only in slope ( $\alpha$ ). The outdoor scene shows a slope of  $-0.98$ , as compared to a slope of  $-1.42$  for the indoor scene.

[Figures 2](#) and [3](#) show the distributions of the slopes of the spatial frequency spectra for the different visual environments under investigation. The three natural image sets, in which no man-made objects were visible, all followed the pattern originally described by Field,<sup>27</sup> with slopes (mean  $\pm$  standard deviation) close to unity:  $-1.06 \pm 0.10$ , Berkeley;  $-0.90 \pm 0.09$ , Texas;  $-1.03 \pm 0.14$ , Botswana. The calculated slopes and 95% confidence intervals (CI) for all of the image categories are summarized in [Table 1](#). For both the Berkeley and Texas datasets, outdoor urban settings showed significantly greater spatial frequency slopes, compared to natural images. Images of indoor settings, which by definition are all man-made environments, showed the steepest slopes, representing the greatest relative loss of high spatial frequencies ( $-1.48 \pm 0.20$ , UCB;  $-1.52 \pm 0.17$ , UT).

As shown in [Table 2](#), the differences between natural outdoor environments and indoor environments are highly significant, statistically ( $P < 0.0001$  in all cases), and consistent across the Berkeley and Texas datasets, despite the very different imaging systems used (mobile phone camera vs. Nikon digital SLR) and with the Texas dataset being collected

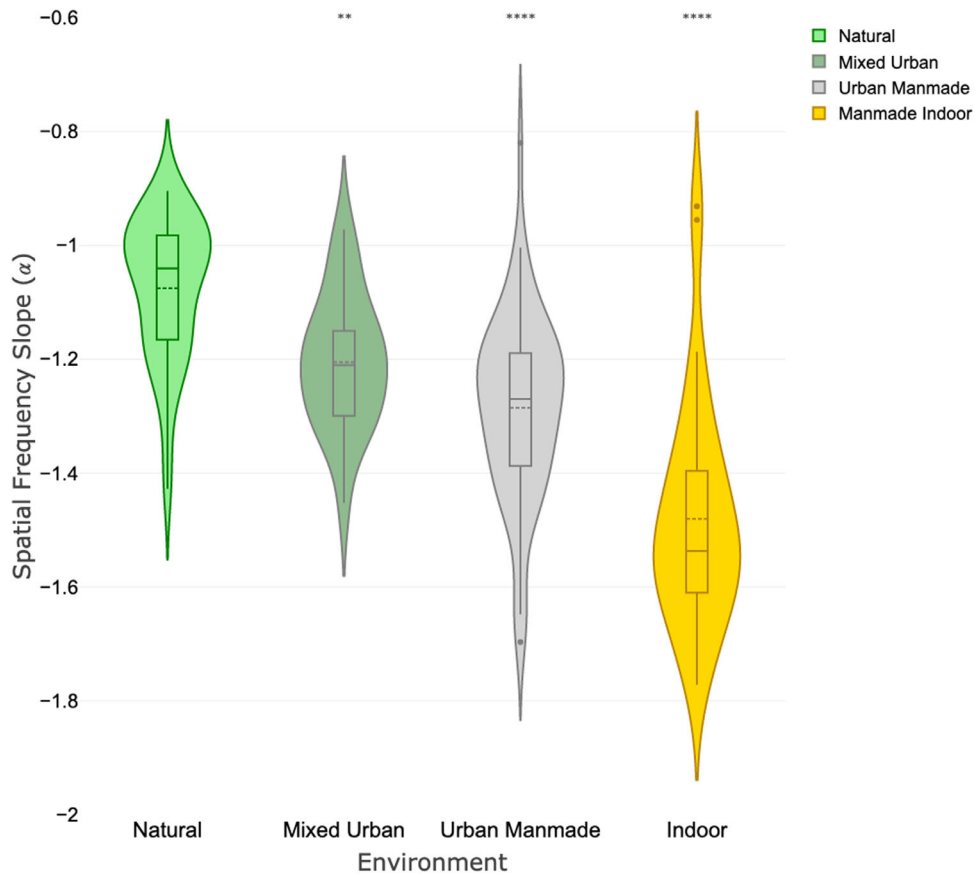


FIGURE 2. Violin plots of the calculated amplitude spectrum slopes ( $\alpha$ ) for the different types of images from the Berkeley image set. Significance markers (\*) indicate comparison with the natural image set.

TABLE 1. Log Amplitude Versus Spatial Frequency Slopes for Different Image Sets and Environments

	<i>N</i>	Mean	Median	SD	SE	Lower 95% CI	Upper 95% CI
Berkeley (UCB)							
Nature	42	-1.08	-1.04	0.12	0.02	-1.11	-1.04
Mixed urban	20	-1.21	-1.21	0.12	0.03	-1.26	-1.15
Outdoor man-made	60	-1.29	-1.27	0.16	0.02	-1.33	-1.24
Indoor man-made	33	-1.48	-1.54	0.20	0.03	-1.55	-1.41
Texas (UT)							
Nature	308	-0.90	-0.88	0.09	0.01	-0.91	-0.89
Campus (mixed)	90	-1.12	-1.11	0.12	0.01	-1.14	-1.10
Outdoor man-made	171	-1.22	-1.21	0.14	0.01	-1.24	-1.20
Indoor man-made	25	-1.52	-1.55	0.17	0.03	-1.59	-1.45
Botswana (UPenn)							
Nature	65	-1.04	-1.02	0.14	0.02	-1.07	-1.00

SD, standard deviation; SE, standard error.

for a purpose unrelated to the current studies' core hypothesis.

### Impact of Bangerter Foil on Spatial Slope of a Natural Image

As noted above, a 0.4 Bangerter foil is sufficient to induce myopia in some animals. Figure 4 shows its impact on the spatial frequency slope of an outdoor image featuring a tree,

as captured with and without a 0.4 Bangerter foil. The unfiltered image has a spatial frequency slope of -0.88, while the same scene photographed through a 0.4 Bangerter foil yielded a spatial frequency slope of -1.47. The latter value is comparable with the slopes derived from indoor images in both the Berkeley dataset (mean slope = -1.48; 95% CI -1.41 to -1.55) and the Texas dataset (mean slope = -1.52; 95% CI -1.45 to 1.59), as described above.

By comparing the FFT spectra of the two images an empirical estimation of the modulation transfer function

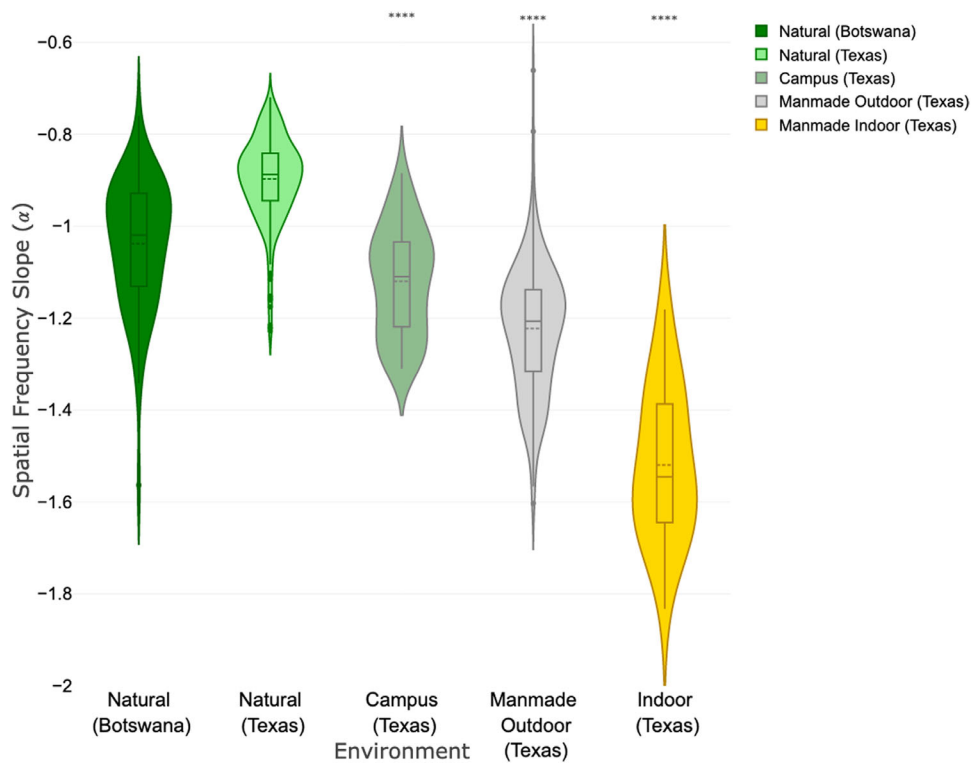


FIGURE 3. Violin plots of the calculated amplitude spectrum slopes ( $\alpha$ ) for the different types of images from the Botswana and Texas image sets. Significance markers (\*) indicate comparison with the Texas natural image set.

TABLE 2. Comparison of Spatial Slope By Image Category (Analysis of Variance, Heteroscedastic Variance Model)

Comparison	Slope ( $\alpha$ )		
	Difference	SE	P Value
Berkeley (UCB)			
Nature vs. mixed urban	-0.13	0.03	0.0014
Nature vs. outdoor man-made	-0.21	0.03	<0.0001
Nature vs. indoor man-made	-0.41	0.04	<0.0001
Texas (UT)			
Nature vs. campus	-0.22	0.01	<0.0001
Nature vs. outdoor man-made	-0.33	0.01	<0.0001
Nature vs. indoor man-made	-0.62	0.03	<0.0001

SE, standard error.

(MTF) of this Bangerter foil was also estimated (Fig. 5). A marked reduction in the amplitude of mid- and high spatial frequencies is evident, with little impact on lower spatial frequencies ( $< 1$  c/deg).

### Relationship of Scene Luminance and Spatial Frequency Content

On account of interest in the impact of illumination on myopia development, illuminance estimates for the various image set environments were also compared. As shown in Figures 6 and 7, indoor versus natural environments were found to show the greatest difference. For the Texas image set the natural outdoor environment has a mean estimated illuminance of 11,200 lux (95% CI 10,000–12,900 lux) compared to 430 lux (95% CI 282–631 lux) for the indoor environment. Comparable values for the Berkeley image set

were 14,100 lux (95% CI 9,120–21,900 lux) and 430 lux (95% CI 245–759 lux), respectively. Indoor environments showed markedly lower illuminance than outdoors, but there were no consistent differences in the outdoor scenes by category.

### DISCUSSION

The analyses reported here demonstrate that urban and indoor environments have different spatial properties compared to natural outdoor environments. In particular, urban and indoor environments are relatively deficient in high spatial frequencies, and the slope of the relationship between spectral amplitude and spatial frequency is steeper (slope of  $-1.50$ ) in such environments when compared to natural settings (slope close to  $-1$ , consistent with the  $1/f$  relationship described by Field).<sup>27</sup> In addition, the spatial frequency characteristics of the indoor environment are comparable to those recorded with a 0.4 Bangerter foil, which has been reported to induce myopia in mammalian animal models. For example, in the guinea pig model, the 0.8 Bangerter foil, which causes minimal image blur image, had no significant effect on eye growth, whereas foils of intermediate density (such as the 0.4 foil used here), induced ~50% to 60% of the amount of FDM induced by a diffuser that precluded all form vision.<sup>22</sup> Although similar trends were reported by Smith et al<sup>23</sup> in a primate model with three grades of Bangerter foils (0.4, 0.1, LP), there was also substantial interanimal variability in responses, with the lighter, 0.4 foil. This indicates that modest reductions in higher spatial frequencies can produce myopic shifts in primates. If humans respond in a similar way, then on the basis of the observed spatial frequency spectrum of the urban and indoor environments measured here, this

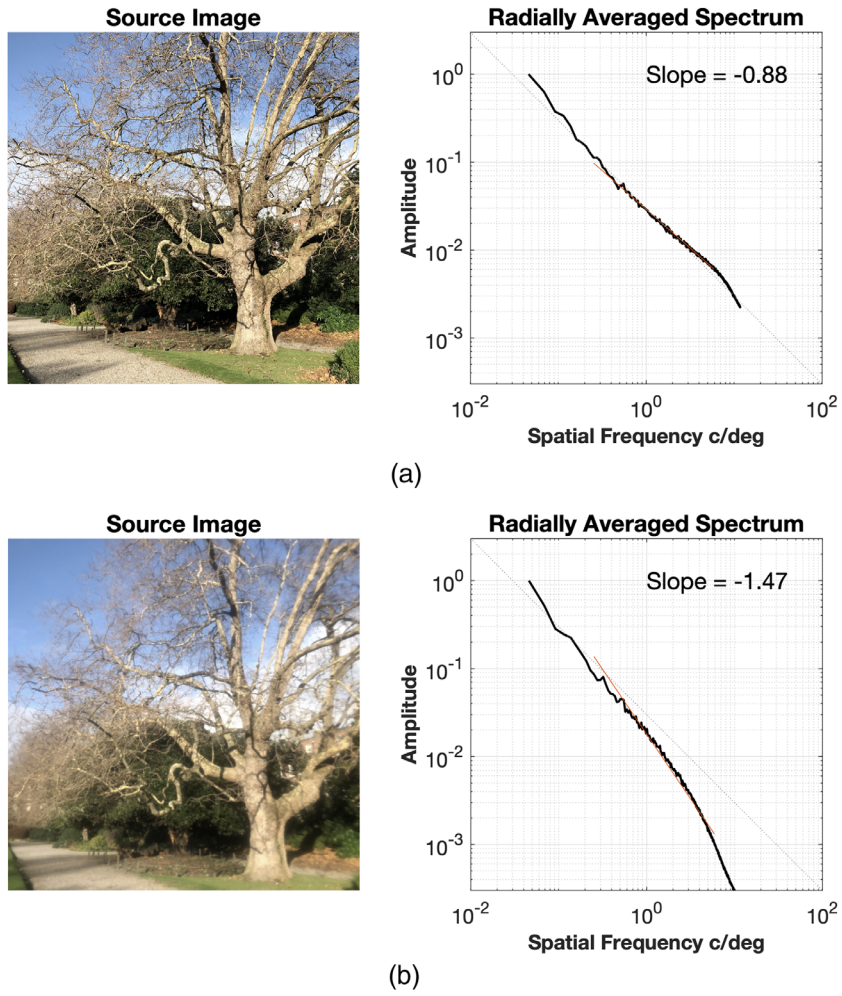


FIGURE 4. Photos taken (a) with and (b) without a 0.4 Bangerter foil and derived amplitude versus spatial frequency spectra.

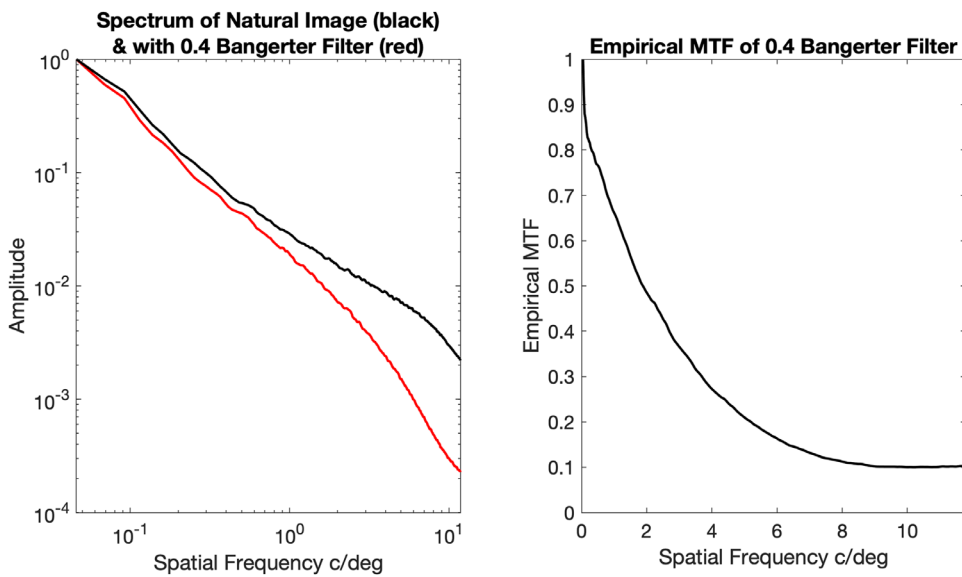


FIGURE 5. Comparison of amplitude vs. spatial frequency spectra corresponding to unfiltered image and image taken through a 0.4 Bangerter foil and the derived empirical MTF.

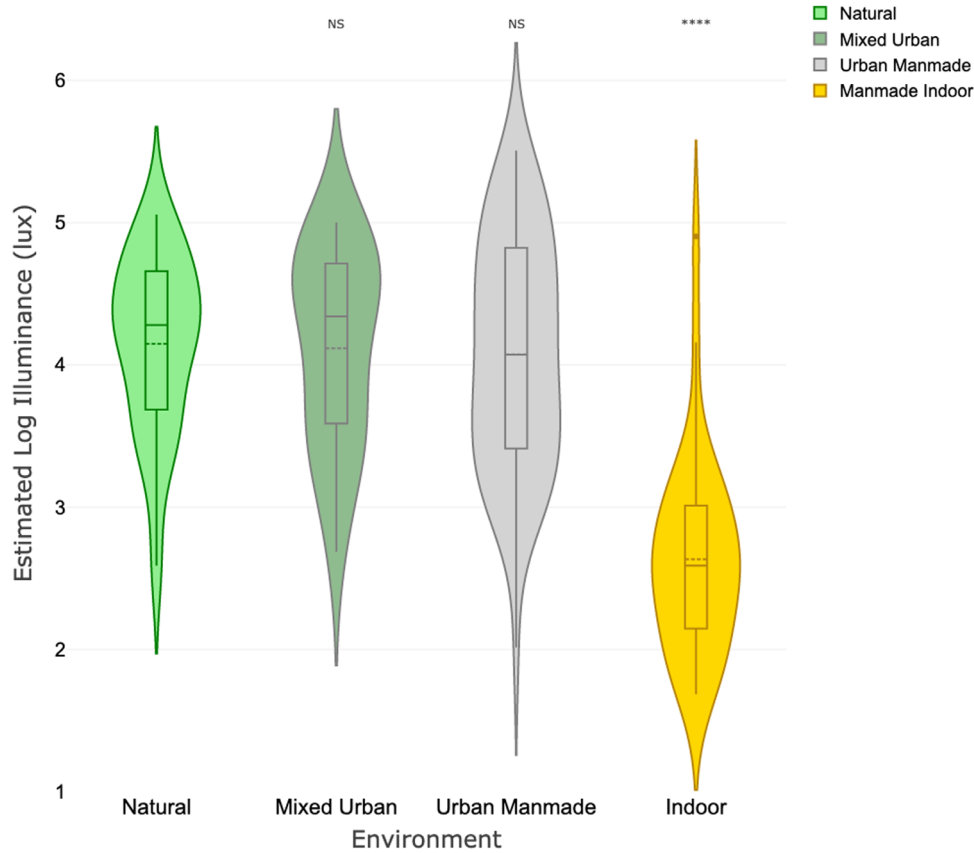


FIGURE 6. Estimated log Illuminance (lux) by category for the Berkeley image set. Significance markers (\*) indicate comparison with the natural image set.

leads to the hypothesis that the such environments may be intrinsically myopigenic, especially when experienced over extended periods.

The present analyses cannot be taken as evidence that the retina is estimating the slope of the relationship between amplitude and spatial frequency in an image, but the animal studies provide support for the hypothesis that the spatial frequency content of the retinal image has an impact on eye growth. Theoretically the determination of whether a retinal image is in focus could be achieved simply by determining contrast at intermediate to high spatial frequencies, as suggested by Hess et al.,<sup>34</sup> and the differences noted between natural and man-made images could also be applicable to such simple models of retinal defocus detection. On the basis that the range of lens powers capable of inducing myopia varies between different species, it is likely that different spatial frequency ranges are involved.<sup>16,20</sup> Investigation of the optical properties of Bangerter foils shows that, like defocus, these preferentially impact higher spatial frequencies. The 0.4 foil reduces the contrast at 2 cycles per degree by approximately 50% and largely eliminates spatial frequencies over 7 cycles per degree.<sup>26</sup> Irrespective of the spatial frequencies that may be involved in controlling eye growth, the scale invariance embodied in the  $1/f^r$  relationship demonstrated in these image sets indicates that natural scenes will display relatively higher amplitudes in higher spatial frequencies than man-made scenes.

If certain visual environments (based on their spatial frequency spectra and hence their retinal image profiles) can act as myopigenic stimuli, the question arises of how such stimuli would interact with optical defocus in relation to regulating eye growth. To date, this question has only been explored in the chick model where a 0.4 foil was found to induce myopia in just two days,<sup>24</sup> whereas it had no effect on the compensatory (inhibitory) growth pattern and hyperopic shift elicited by positive lenses (+6 D).<sup>35</sup> However, with the latter lens-foil combination, the choroidal contribution to the compensatory response was much reduced, even while eyes compensated in the appropriate direction overall.<sup>24</sup> That the choroidal response appears to be more sensitive than the scleral response to the degrading effects of the Bangerter foils, raises the possibility of different underlying regulatory signal pathways, at least in the case of compensation to myopic defocus.

The myopia-inducing effect of negative defocusing lenses (hence, hyperopic defocus) on eye growth can be suppressed by relatively short periods of uninterrupted vision in a range of species,<sup>36-38</sup> suggesting that an in-focus (sharp) retinal image can act as a reset or stop signal. These animal studies raise the, as yet unanswered, question of whether high spatial frequency reductions induced by 0.4 Bangerter foils can limit the effectiveness of such a stop signal. In considering how these findings may apply to human myopia, our observation that man-made environments may be severely deficient in high spatial frequency



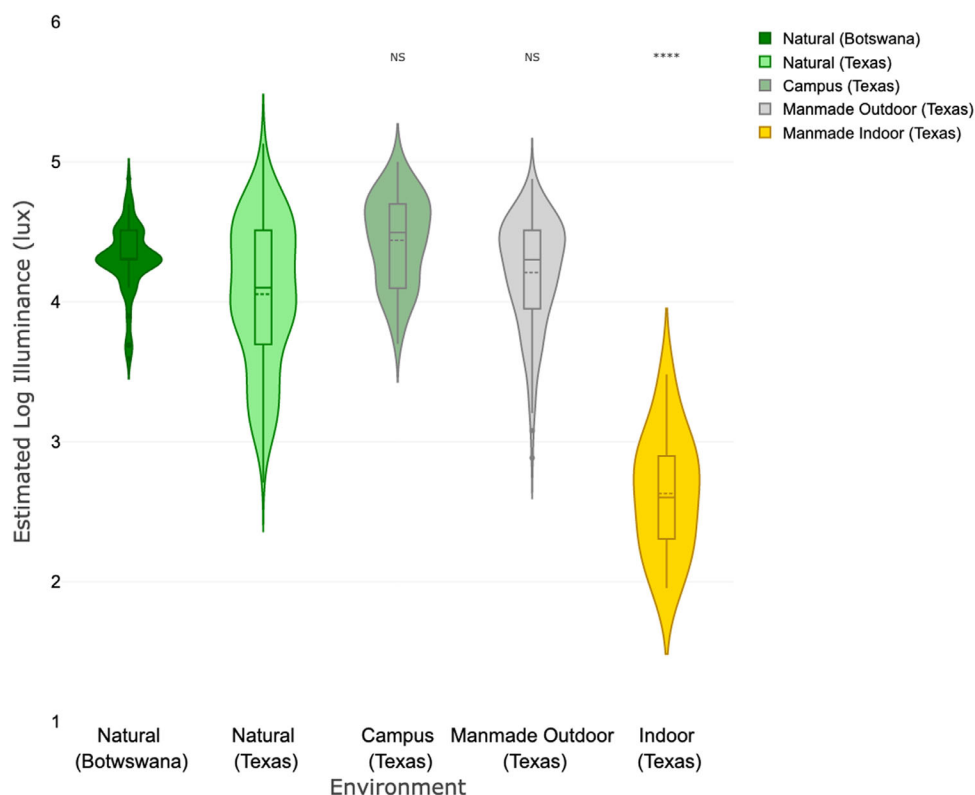


FIGURE 7. Estimated log Illuminance (lux) by category for the Botswana and Texas image sets. Significance markers (\*) indicate comparison with the Texas natural image set.

information suggests that such visual environments may potentially both activate the retinal mechanism underlying deprivation myopia and interfere with the retinal stop signaling pathways.

Conversely, enhancing spatial frequency content of the visual scene may help to limit myopia. On the basis of animal studies, short but not brief periods of “normal” retinal stimulation would be expected to be beneficial in humans. In chicks 30 and 130 minutes of uninterrupted, normal vision per day can reduce FDM by 50% and 95%, respectively.<sup>25</sup> In primates, one hour of normal vision reduced FDM by 50%, and four hours unrestricted vision effectively eliminated it.<sup>39</sup> This leads to the testable hypothesis that enhancing the spatial frequency properties of the urban and indoor environments may assist in reducing myopia development. In urban settings, this could be done outdoors with additional planting in urban settings. As demonstrated in this article, mixed urban images with greenery and buildings had a significantly higher spatial frequency slopes, than urban scenes lacking any greenery. Indoors, application of wall papers with natural scenes, for example, inside schools may help to provide a “normal” pattern of spatial frequency. However, more research is necessary to confirm this hypothesis

The findings presented here may also have relevance to the largely unexplained association between myopia and urban environments.<sup>6,7</sup> Man-made outdoor environments showed spatial frequency properties that were intermediate between natural outdoor scenes and indoor environments. The differences in the spatial properties of natural and urban outdoor scenes were statistically significant. The spatial frequency composition of the constructed

environment, both indoors and outdoors, is therefore different from the natural world. The two-dimensional FFT spectra shown above, also revealed orientational differences. It has been proposed that the man-made environment shows more spatial anisotropy (i.e., orientation-dependent spatial differences) and that this may alter visual perception. Referred to as the “carpentered environment” hypothesis,<sup>40</sup> it is not a consistent finding and appears to be spatial frequency dependent.<sup>41</sup> In addition, orientation selectivity is a well-known feature of cortical neurons but rare in retinal receptive fields.<sup>42</sup> Nevertheless, in light of how little we know about how the retina extracts information relevant to eye growth regulation from retinal images, such aspects of the spatial environment merit further investigation. In addition, this analysis is limited in that it analyzed static rather than dynamic images typical of our natural visual world which could vary in illuminance and spatial frequency content—variations that may be important to eye growth. Nevertheless, the original observation of Field and the result of this study show that while images may vary dramatically, the frequency spectra are remarkably constant. Exploring an indoor or urban environment will, on the basis of our findings, produce very little exposure to a natural spatial frequency spectrum.

Although time outdoors has been shown to be beneficial in relation to myopia development,<sup>3</sup> potential indoor factors that may contribute to myopia remain unidentified. Based on our results, we suggest that the reduced high spatial content of the visual environment may be a contributing factor. Although this analysis attempted to characterize the spatial features of the indoor environment, our study did not examine the dioptric variation of the indoor

environment that has been proposed as another contributory factor in myopia development.<sup>13</sup> Furthermore, the greatest reductions in spatial frequency are observed indoors where illuminance is much lower than outdoors, suggesting that the spatial frequency content of outdoor environments may be an uncontrolled, confounding variable in studies that have only considered light exposure as a protective factor for myopia development. It is worth noting that the spatial frequency content of an image is intrinsically and computationally independent of illuminance. This is demonstrated in these results in that no difference in estimated scene illuminance was found between natural and man-made outdoor environments (Figs. 6 and 7), but these two settings showed significant differences in spatial frequency content (Figs. 2 and 3).

In relation to the potential role of bright light in protecting against myopia, one finding from animal studies has proven difficult to equate to human myopia. High illuminance levels strongly inhibit the development of form deprivation in chickens<sup>43</sup> and primates,<sup>44</sup> yet similar light levels were found to be without effect on lens-induced myopia in primates.<sup>45</sup> If we assume that the spatial frequency characteristics of man-made environments act in humans in a similar way to that inferred from the animal bright light studies, we hypothesize that the beneficial effects of high light levels outdoors are manifest through blocking the form deprivation signaling pathway in outdoor environments with reduced high spatial frequencies (e.g., urban settings). To date, this hypothesis has not been directly tested in animal studies, i.e., by determining whether bright light can inhibit form deprivation induced by Bangerter foils. Although attention has been given to increasing light levels in classrooms,<sup>46</sup> enhancing the spatial frequency content of the indoor classroom environment with appropriate wall and ceiling coverings may provide an alternative, simple myopia control intervention, in effect removing the myopic stimulus rather than blocking it.

## CONCLUSION

Compared to the spatial properties of the natural world, man-made environments have spatial features similar to those than created by diffusing filters that induce form deprivation myopia in animal models. From the perspective of what has been learned about local retinal guidance of eye growth in animal models, form deprivation myopia may be one of the missing drivers of the human myopia epidemic, with a potential solution being the enrichment of the indoor environment with higher spatial frequencies to mimic the spatial properties of natural, outdoor environments.

## Acknowledgments

Disclosure: **D.I. Flitcroft**, None; **E.N. Harb**, None; **C.F. Wildsoet**, None

## References

- Holden BA, et al. Global Prevalence of Myopia and High Myopia and Temporal Trends from 2000 through 2050. *Ophthalmology*. 2016;123:1–7.
- Huang H-MM, et al. The association between near work activities and myopia in children - A systematic review and meta-analysis. *PLoS One*. 2015;10:1–15.
- Xiong S, et al. Time spent in outdoor activities in relation to myopia prevention and control: a meta-analysis and systematic review. *Acta Ophthalmol*. 2017;95:551–566.
- Harb EN, Wildsoet CF. Origins of Refractive Errors: Environmental and Genetic Factors. *Annu Rev Vis Sci*. 2019;5:47–72.
- Cao K, Wan Y, Yusufu M, Wang N. Significance of Outdoor Time for Myopia Prevention: A Systematic Review and Meta-Analysis Based on Randomized Controlled Trials. *Ophthalmic Res*. 2020;63:97–105.
- He M, Zheng Y, Xiang F. Prevalence of myopia in urban and rural children in mainland china. *Optometry and Vision Science*. 2009;86:40–44.
- Ip JM, Rose KA, Morgan IG, Burlutsky G, Mitchell P. Myopia and the urban environment: findings in a sample of 12-year-old Australian school children. *Invest Ophthalmol Vis Sci*. 2008;49:3858–63.
- Zhang M, et al. Population Density and Refractive Error among Chinese Children. *Investig Ophthalmology Vis Sci*. 2010;51:4969.
- Wu X, et al. Housing type and myopia: The mediating role of parental myopia. *BMC Ophthalmol*. 2016;16:1–7.
- Hagen LA, et al. Prevalence and Possible Factors of Myopia in Norwegian Adolescents. *Sci Rep*. 2018;8:1–10.
- Wu PC, et al. Myopia Prevention and Outdoor Light Intensity in a School-Based Cluster Randomized Trial. *Ophthalmology*. 2018;125:1239–1250.
- Ngo C, Saw SM, Dharani R, Flitcroft I. Does sunlight (bright lights) explain the protective effects of outdoor activity against myopia? *Ophthalmic Physiol Opt*. 2013;33:368–372.
- Flitcroft DI. The complex interactions of retinal, optical and environmental factors in myopia aetiology. *Prog Retin Eye Res*. 2012;31:622–60.
- Rose KA, et al. Outdoor Activity Reduces the Prevalence of Myopia in Children. *Ophthalmology*. 2008;115:1279–1285.
- Thorn F, Cruz A, Machado A, Carvalho R. Refractive status of indigenous people in the north western Amazon region of Brazil. *Optom Vis Sci*. 2005;82:267–72.
- Troilo D, et al. IMI-Report on Experimental Models of Emmetropization and Myopia. *Invest Ophthalmol Vis Sci*. 2019;60:M31–M88, doi:10.1167/iovs.18-25967.
- Flitcroft DI. Emmetropisation and the aetiology of refractive errors. *Eye*. 2014;28:169–179.
- Flitcroft DI. Is myopia a failure of homeostasis? *Exp Eye Res*. 2013;114:16–24.
- Zadnik K, Mijiti DO. How applicable are animal myopia models to human juvenile onset myopia? *Vision Res*. 1995;35:1283–1288.
- Flitcroft DI. The lens paradigm in experimental myopia: oculomotor, optical and neurophysiological considerations. *Ophthalmic Physiol Opt*. 1999;19:103–111.
- Bartmann M, Schaeffel F. A simple mechanism for emmetropization without cues from accommodation or colour. *Vision Res*. 1994;34:873–876.
- Bowrey HE, Metse AP, Leotta AJ, Zeng G, Mcfadden SA. The relationship between image degradation and myopia in the mammalian eye. *Clin Exp Optom*. 2015;98:555–563.
- Smith EL, Hung LF. Form-deprivation myopia in monkeys is a graded phenomenon. *Vision Res*. 2000;40:371–381.
- McLean RC, Wallman J. Severe astigmatic blur does not interfere with spectacle lens compensation. *Investig Ophthalmol Vis Sci*. 2003;44:449–457.
- Tran N, Chiu S, Tian Y, Wildsoet CF. The significance of retinal image contrast and spatial frequency composition for eye growth modulation in young chicks. *Vision Res*. 2008;48:1655–62.
- Pérez GM, Archer SM, Artal P. Optical characterization of bangerter foils. *Investig Ophthalmol VisSci*. 2010;51:609–613.

27. Field DJ. Relations between the statistics of natural images and the response properties of cortical cells. *J Opt Soc Am A*. 1987;4:2379–2394.
28. Tolhurst DJ, Tadmor Y, Chao T. Amplitude spectra of natural images. *Ophthalmic Physiol Opt*. 1992;12:229–32.
29. Peitgen H-O, Saupe D, Barnsley MF, Michael F. & Science, T. *The Science of Fractal Images*. Springer-Verlag;1988.
30. Burge J, Geisler WS. Optimal defocus estimation in individual natural images. *Proc Natl Acad Sci*. 2011;108:16849–16854.
31. Geisler WS, Perry JS. Statistics for optimal point prediction in natural images. *J Vis*. 2011;11–14, doi:[10.1167/11.12.14](https://doi.org/10.1167/11.12.14).
32. Tkačik G, et al. Natural images from the birthplace of the human eye. *PLoS One*. 2011;6:e20409, doi:[10.1371/journal.pone.0020409](https://doi.org/10.1371/journal.pone.0020409).
33. Ray SF. *Applied Photographic Optics*, 3rd ed. Focal Press;2002.
34. Hess RF, Schmid KL, Dumoulin SO, Field DJ, Brinkworth DR. What Image Properties Regulate Eye Growth? *Curr Biol*. 2006;16:687–691.
35. Park TW, Winawer J, Wallman J. Further evidence that chick eyes use the sign of blur in spectacle lens compensation. *Vision Res*. 2003;43:1519–31.
36. Schmid KL, Wildsoet CF. Effects on the compensatory responses to positive and negative lenses of intermittent lens wear and ciliary nerve section in chicks. *Vision Res*. (1996), doi:[10.1016/0042-6989\(95\)00191-3](https://doi.org/10.1016/0042-6989(95)00191-3).
37. Winawer J, Wallman J. Temporal constraints on lens compensation in chicks. *Vision Res*. 2002;42:2651–68.
38. Kee C, et al. Temporal Constraints on Experimental Emmetropization in Infant Monkeys. *Investig Ophthalmology Vis Sci*. 2007;48:957.
39. Smith EL, Hung LF, Kee CS, Qiao Y. Effects of brief periods of unrestricted vision on the development of form-deprivation myopia in monkeys. *Investig Ophthalmol Vis Sci*. 2002;43:291–299.
40. Segall MH, Campbell DT, Herskovits MJ. *The Influence of Culture on Visual Perception by Donald T. Campbell and Melville J. Herskovits*, copyright © 1966 by The Bobbs-Merrill Company, Inc. The Bobbs-Merrill Company, Inc.;1966.
41. Switkes E, Mayer MJ, Sloan JA. Spatial frequency analysis of the visual environment: Anisotropy and the carpentered environment hypothesis. *Vision Res*. 1978;18:1393–1399.
42. Antinucci P, Hindges R. Orientation-Selective Retinal Circuits in Vertebrates. *Front. Neural Circuits*. 2018;12:11.
43. Ashby RS, Schaeffel F. The Effect of Bright Light on Lens Compensation in Chicks. *Investig Ophthalmology Vis Sci*. 2010;51:5247.
44. Smith EL, Hung L-F, Huang J, Huang J. Protective effects of high ambient lighting on the development of form-deprivation myopia in rhesus monkeys. *Invest Ophthalmol Vis Sci*. 2012;53:421–8.
45. Smith EL, Hung L-F, Arumugam B, Huang J, Huang J. Negative lens-induced myopia in infant monkeys: effects of high ambient lighting. *Invest Ophthalmol Vis Sci*. 2013;54:2959–69.
46. Zhou Z, et al. Pilot study of a novel classroom designed to prevent myopia by increasing children's exposure to outdoor light. *PLoS One*. 2017;12:e0181772, doi:[10.1371/journal.pone.0181772](https://doi.org/10.1371/journal.pone.0181772).